



UNIVERSITÀ  
DEGLI STUDI  
FIRENZE

# FLORE

## Repository istituzionale dell'Università degli Studi di Firenze

### **ED-XRF set-up for size-segregated aerosol samples analysis**

Questa è la Versione finale referata (Post print/Accepted manuscript) della seguente pubblicazione:

*Original Citation:*

ED-XRF set-up for size-segregated aerosol samples analysis / V. Bernardoni; E. Cuccia; G. Calzolai; M. Chiari; F. Lucarelli; D. Massabo; S. Nava; P. Prati; G. Valli; R. Vecchi. - In: X-RAY SPECTROMETRY. - ISSN 0049-8246. - STAMPA. - 40:(2011), pp. 79-87. [10.1002/xrs.1299]

*Availability:*

This version is available at: 2158/495657 since: 2017-10-16T17:36:41Z

*Published version:*

DOI: 10.1002/xrs.1299

*Terms of use:*

Open Access

La pubblicazione è resa disponibile sotto le norme e i termini della licenza di deposito, secondo quanto stabilito dalla Policy per l'accesso aperto dell'Università degli Studi di Firenze (<https://www.sba.unifi.it/upload/policy-oa-2016-1.pdf>)

*Publisher copyright claim:*

(Article begins on next page)

# ED-XRF set-up for size-segregated aerosol samples analysis

Vera Bernardoni,<sup>a\*</sup> Eleonora Cuccia,<sup>b</sup> Giulia Calzolari,<sup>c</sup> Massimo Chiari,<sup>c</sup> Franco Lucarelli,<sup>c</sup> Dario Massabò,<sup>b</sup> Silvia Nava,<sup>c</sup> Paolo Prati,<sup>b</sup> Gianluigi Valli<sup>a</sup> and Roberta Vecchi<sup>a</sup>

The knowledge of size-segregated elemental concentrations in atmospheric particulate matter (PM) gives a useful contribution to the complete chemical characterisation; this information can be obtained by sampling with multi-stage cascade impactors. In this work, samples were collected using a low-pressure 12-stage Small Deposit Impactor and a 13-stage rotating Micro Orifice Uniform Deposit Impactor<sup>TM</sup>. Both impactors collect the aerosol in an inhomogeneous geometry, which needs a special set-up for X-ray analysis. This work aims at setting up an energy dispersive X-ray fluorescence (ED-XRF) spectrometer to analyse quantitatively size-segregated samples obtained by these impactors. The analysis of cascade impactor samples by ED-XRF is not customary; therefore, as additional consistency test some samples were analysed also by particle-induced X-ray emission (PIXE), which is more frequently applied to size-segregated samples characterised by small PM quantities. A very good agreement between ED-XRF and PIXE results was obtained for all the detected elements in samples collected with both impactors. The good inter-comparability proves that our methodology is reliable for analysing size-segregated samples by ED-XRF technique. The advantage of this approach is that ED-XRF is cheaper, easier to use, and more widespread than PIXE, thus promoting an intensive use of multi-stage impactors. Copyright © 2011 John Wiley & Sons, Ltd.

## Introduction

Particulate matter (PM) has great impact on environment and human health. Indeed, many epidemiological studies have shown a correlation between the increase of PM concentration and morbidity and/or mortality.<sup>[1–3]</sup> Several countries routinely monitor PM in terms of daily average mass concentration of PM10 and PM2.5 (i.e. mass concentration of atmospheric particles with aerodynamic diameter smaller than 10 and 2.5  $\mu\text{m}$ , respectively) according to current legislation. In some cases, samples collected for regulatory purposes are also analysed to determine their chemical composition.

The detailed knowledge of aerosol properties as a function of size and time is of great concern in studies on radiative and health effects of atmospheric particles.<sup>[4,5]</sup> Moreover, size-segregated chemical speciation of atmospheric aerosol provides very useful information on its formation processes, residence times, and emission sources.

Atmospheric PM is a complex mixture of organic and inorganic compounds,<sup>[6]</sup> which originate from a number of anthropogenic (e.g. combustion processes, industrial activities, traffic) and natural (e.g. soil, vegetation, sea spray) sources. Among the large number of chemical species in aerosol samples, elements are important trace constituents because they can be toxic for human beings and are markers for specific emission sources.<sup>[7]</sup>

Size-segregated samples are usually collected in the 0.01–10  $\mu\text{m}$  range by multi-stage cascade impactors.<sup>[8–10]</sup> Except few instruments (e.g. streaker sampler,<sup>[11]</sup> Davis Rotating Uniform size-cut Monitor (DRUM)<sup>[12,13]</sup>, and Rotating Drum Impactor (RDI)<sup>[14]</sup>), impactors are generally not suitable to obtain long temporal series in polluted sites, because samplings last short periods (1 day or less to avoid heavy loadings on the impaction foils)<sup>[15]</sup> and the impaction foils have to be manually changed.

The chemical characterisation of size-segregated samples can be performed by different techniques such as inductively coupled plasma mass spectrometry<sup>[16]</sup> for elemental composition and ion chromatography<sup>[17]</sup> for inorganic ion analysis. Both techniques need the sample pre-treatment and are completely destructive.

Powerful techniques to detect elements are those based on the analysis of fluorescence X-rays emitted after excitation by charged particles [e.g. particle-induced X-ray emission (PIXE)]<sup>[18]</sup> or X-rays [e.g. energy dispersive X-ray fluorescence (ED-XRF)].<sup>[19]</sup> The advantages of these techniques are that they do not need any sample pre-treatment and are not destructive. A major drawback of PIXE is the need for an accelerator facility, which is not readily available and gives usually a limited beam time.

ED-XRF spectrometry had been rarely<sup>[20,21]</sup> applied to size-segregated samples because they are often inhomogeneous and/or with a multi-spot geometry, which complicates direct X-ray quantitative analysis. Nevertheless, ED-XRF spectrometry in this application is of interest because it is a widespread, cheap, and user-friendly technique.

The aim of our work was to set up an ED-XRF spectrometer for the elemental analysis of aerosol samples collected by two different impactors. Indeed, two identical spectrometers (ED2000,

\* Correspondence to: Vera Bernardoni, Department of Physics, Università degli Studi di Milano and INFN, Via Celoria 16, 20133 Milano, Italy.  
E-mail: vera.bernardoni@unimi.it

a Department of Physics, Università degli Studi di Milano and INFN, 20133 Milano, Italy

b Department of Physics, Università di Genova and INFN, 16146 Genova, Italy

c Department of Physics and Astronomy, Università di Firenze and INFN, 50019 Sesto Fiorentino, Italy

Oxford Instruments) operate in the laboratories of the Universities of Genoa and Milan, which use a rotating nano-Micro Orifice Uniform Deposit Impactor (nano-MOUDI™ by MSP Corporation, USA) and a small deposit impactor (SDI by Dekati Ltd., Finland), respectively. Opposite to the case described in the literature,<sup>[20]</sup> these impactors collect inhomogeneous samples with a different deposition pattern in each stage; therefore, a careful measurement of the X-ray yield on the irradiated area was mandatory.

In this work, the exciting beam characteristics were explored to choose suitable irradiation conditions. The ED-XRF sensitivity curve for each spectrometer was determined to quantify elemental concentrations on the samples collected by the two multi-stage cascade impactors. As a further quality check, an inter-comparison between ED-XRF and PIXE results was carried out.

The results reported in this article refer to two specific impactors, but the methodology can be generalised to any impactor sample with inhomogeneous and/or multi-spot geometry.

## Instrumentation

### Sampling devices

In this work, two multi-stage cascade impactors (a 12-stage SDI and a 13-stage rotating nano-MOUDI™) were used. Both devices collect size-segregated aerosol samples in the range between tens of nanometres and about 10 µm (see specific details for each model in the following). The cut-off at low-size diameters is obtained using reduced pressure and high jet velocities.<sup>[8]</sup>

The low-pressure SDI is a 12-stage impactor,<sup>[10]</sup> which has cut-off diameters nominally ranging from 0.045 to 8.5 µm (in our impactor real cut-off diameters are 0.0479, 0.0897, 0.1548, 0.235, 0.349, 0.598, 0.804, 1.07, 1.68, 2.70, 4.12, and 8.57 µm). It operates at 11 l min<sup>-1</sup> with 135 mbar in the lowest stage.

Samples were collected on coated Kapton® foils (actually, other materials as thin polycarbonate films can also be used), which were supported by 25 mm plastic rings. Aerosol particles are collected in non-uniform, multi-spot, point-like deposits enclosed in an 8 mm diameter area (Fig. 1a).

The rotating nano-MOUDI™ (Model 125-R 13-stage MOUDI II) is a 13-stage impactor, with nominal cut-off diameters ranging from 0.010 to 10 µm (actual cut-off diameters are 0.010, 0.018, 0.032, 0.056, 0.10, 0.18, 0.32, 0.56, 1.0, 1.8, 3.2, 5.6, and 10 µm). It operates at 10 l min<sup>-1</sup>.

Samples were collected on 47-mm diameter polycarbonate filters (Nuclepore™, pore size 0.4 µm). Opposite to SDI foils, which are sold already coated, polycarbonate filters were coated in the Genoa laboratory using the Dekati DS-515 spray. Filters were placed in a home-made mask to spray a 36-mm diameter area on the filter. Filters were sprayed twice with a 20-min interval. The average thickness of polycarbonate filters was about 850 µg cm<sup>-2</sup>, while the coating thickness was about 100 µg cm<sup>-2</sup>. Because of the continuous rotation of the impaction stages, sample deposits are circular and concentric (Fig. 1b) and they are enclosed in a 16-mm diameter area, except for the three lowest stages whose diameters are up to 20 mm.

### Analytical techniques

#### ED-XRF spectrometry

ED-XRF measurements were carried out at the Physics Departments of the Universities of Genoa and Milan, where two identical

ED-2000 spectrometers by Oxford Instruments are available and X-ray spectrometry on aerosol samples has been carried out routinely.<sup>[22,23]</sup> In this instrument, the primary X-ray beam is produced by a Coolidge tube ( $I_{\max} = 1$  mA,  $HV_{\max} = 50$  kV) with an Ag anode. The beam spot impinging on the sample is elliptic and its area depends on the collimator mounted on the tube side. A Si (Li) detector with energy resolution better than 145 eV full width at half maximum (FWHM) at 5.9 keV detects X-rays. XRF spectra are fitted using the AXIL software package.<sup>[24]</sup>

The spectrometer in the University of Milan was optimised for analysis of SDI samples. The standards for the sensitivity curve determination were suitably cut from MICROMATTER™ standards (see Section on Set-up for SDI Samples and Inter-comparison with PIXE).

The spectrometer in the University of Genoa was set up for nano-MOUDI samples analysis. The calibration was carried out using a secondary multi-elemental standard, suitably realised for this application (see Section on Set-up for nano-MOUDI™ samples and inter-comparison with PIXE).

#### PIXE set-up

PIXE measurements were performed at the 3-MV Tandatron accelerator of INFN-LABEC (Istituto Nazionale di Fisica Nucleare – Laboratorio di tecniche nucleari per i Beni Culturali, National Institute of Nuclear Physics – Laboratory of Nuclear Techniques for Cultural Heritage) in Florence, where an external beam line is fully devoted to analysis of aerosol samples. Protons of 3.06 MeV in vacuum energy (corresponding to 2.91 MeV on the target) were used as incident beam, with a current intensity of about 10 nA (average value). Measurement time was typically 1200 s sample<sup>-1</sup>. The beam was de-focused and collimated to obtain a homogeneous  $2 \times 1$  mm<sup>2</sup> spot on the target; suitable scanning modes for the two kinds of samples were set up in order to analyse uniformly the sampled area. X-rays were collected by two detectors, a silicon drift detector for light elements (Na–Ca), and a Si(Li) optimised for the detection of X-rays approximately in the range of 4–30 keV (Ti–Pb); energy resolutions were 145 and 190 eV FWHM at 5.9 keV, respectively. The experimental set-up is described in detail elsewhere.<sup>[25]</sup>

The sensitivity curve was determined using MICROMATTER™ standards available at the laboratory. The minimum detection limits (MDLs) were calculated as  $3\sqrt{Cts_b}$ , where  $Cts_b$  is the counts area corresponding to each element (at 1 FWHM) in the blank spectrum. PIXE spectra were analysed using the GUPIX software.<sup>[26]</sup>

## XRF Spectrometer Set-Up and Validation

In a previous work,<sup>[27]</sup> an inter-comparison among PIXE analysis performed in Florence and ED-XRF results obtained in Milan and Genoa had been carried out on homogeneous 24-h aerosol samples (47-mm diameter) and a very good agreement had been obtained.

Nevertheless, the usual ED-XRF configurations were not suitable for analysing cascade impactor samples and new settings were developed. Indeed, the X-ray beam profile is generally not uniform<sup>[28]</sup> and the impactor samples are inhomogeneous and/or with a multi-spot geometry but the aerosol deposits on all stages are enclosed in a defined circular area (in the following called 'enclosing area'). To perform a quantitative XRF analysis of these aerosol samples, a condition where the system response is the

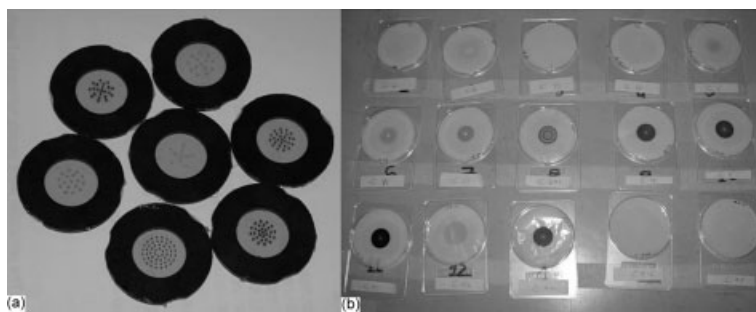


**Figure 1.** Examples of: (a) SDI deposits collected on Kapton<sup>®</sup> foils (stages 1–7) and (b) nano-MOUDI<sup>™</sup> deposits collected on polycarbonate filters (all stages + two blanks).

same for all the points in the enclosing area should be found out. In this condition, the sample can be considered as homogeneously distributed inside it and the analysis of the deposition patterns, which are different for each stage, does not require any particular correction.

Up to now, the ED-XRF set-up has been validated for 'medium-Z' elements ( $Z > 15$ ) at both laboratories. For low-Z elements, work is still in progress in Milan (for results obtained in Genoa see Section on Set-up for nano-MOUDI<sup>™</sup> Samples and Inter-comparison with PIXE) to improve the spectrometer calibration and calculate the self-absorption factors. The latter depend on particles size and deposition thickness<sup>[29]</sup> so that they can strongly vary in different impaction stages.

The set-up procedure was based on the following steps for both SDI and nano-MOUDI samples:

1. Identification of the irradiated area in different geometric conditions using GAFCHROMIC<sup>®</sup> dosimetry films; in detail, 4, 8, 10, 12, and 14 mm diameter collimators (some of which designed for this work) were placed on the X-ray tube side and tested.
2. Scanning of the irradiated area using a point-like probe material to evaluate the contribution given by different points in the sample to the total counts and to find the uniformity area.
3. Determination of the sensitivity curve using suitable elemental standards.
4. Inter-comparison between ED-XRF and PIXE analyses on real size-segregated samples.

The final ED-XRF settings to analyse the samples collected by the two different cascade impactors will be described in detail in the following.

#### Set-up for SDI samples and inter-comparison with PIXE

For the SDI foils, the irradiated area was identified by GAFCHROMIC<sup>®</sup> films and scanned (with a  $1 \times 1 \text{ mm}^2$  spatial resolution) with a Ca point-like probe material. This procedure evidenced that a 10-mm collimator on the X-ray tube and an 8-mm collimator on the detector were those giving a 20% uniformity in Ca counts in an area of 8-mm diameter at least. After having identified the uniformity area, sample holders to ensure reproducible positioning of the samples in this area were realised. To this aim, a mixed cellulose esters filter (Millipore, AAWP type, pore size  $0.8 \mu\text{m}$ ) was punched (hole diameter 8 mm) and suitably marked (Fig. 2) to act as sample holder. This blank sample holder was irradiated to account for its contribution to the background X-ray spectrum.

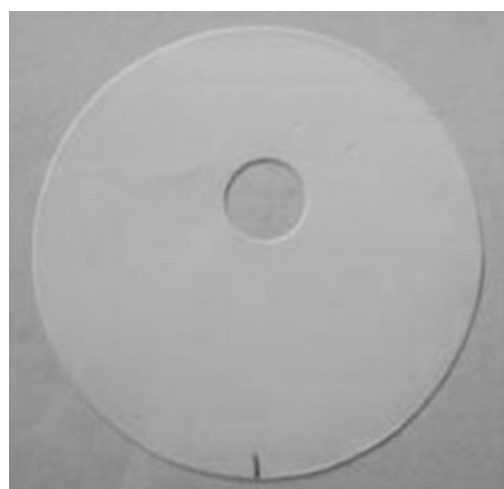


**Figure 2.** Mixed cellulose ester sample holder for standard and sample positioning in the ED-XRF system with the SDI configuration.

MICROMATTER<sup>™</sup> standards were used to obtain the sensitivity curve. They are mono- or multi-elemental standards consisting of thin depositions on 47-mm diameter polycarbonate filters. They are certified within 5% and – in our case – contain two elements at most to avoid secondary fluorescence phenomena. The standard samples were punched for obtaining an 8.8-mm diameter area to be positioned on the 8-mm hole in the sample holder. Then, they were analysed taking into account the possible X-rays attenuation in the small part of the standard covered by the sample holder. The sensitivity curve was validated analysing the SRM2783 standard (air particulate on filter media certified by the NIST, National Institute for Standard and Technology) suitably punched to an 8.8-mm diameter area. MDLs for polycarbonate filters (NIST blanks) were evaluated in  $\mu\text{g sample}^{-1}$  according to the same methodology already described for PIXE (Table 1). In Fig. 3, the comparison between measured and certified concentrations for the NIST standard is given, after blank correction. It is noteworthy that all the elements with concentration higher than MDL (K, Ca, Ti, Cr, Fe, Ni, Cu, Zn, and Pb) showed a good agreement between measured and certified concentrations. An exception was Mn, but the reason for this disagreement is not yet completely clear (see also Section Discussion).

The analysis of the coated Kapton<sup>®</sup> foils used in SDI sampling was carried out by separating the foils from the supporting rings using a cutter: this was necessary to avoid contaminations in the

**Table 1.** MDL for SDI and nano-MOUDI™ configurations

|    | ED-XRF SDI configuration                  |  | PIXE SDI configuration                       | ED-XRF nano-MOUDI configuration                    | PIXE nano-MOUDI configuration                      |
|----|---|--|--|--|--|
|    | MDL NIST<br>( $\mu\text{g sample}^{-1}$ ) | MDL Kapton®<br>( $\mu\text{g sample}^{-1}$ ) | MDL Kapton®<br>( $\mu\text{g sample}^{-1}$ ) | MDL polycarbonate<br>( $\mu\text{g sample}^{-1}$ ) | MDL polycarbonate<br>( $\mu\text{g sample}^{-1}$ ) |
| Na | Not measured                              | Not measured                                 | Not measured                                 | 0.056  | 0.091  |
| Mg | Not measured                              | Not measured                                 | Not measured                                 | 0.020  | 0.078  |
| Al | Not measured                              | Not measured                                 | Not measured                                 | 0.004  | 0.068  |
| Si | Not measured                              | Not measured                                 | Not measured                                 | 0.003  | 0.060  |
| P  | Not measured                              | Not measured                                 | Not measured                                 | 0.002  | 0.047  |
| S  | 0.049                                     | 0.065  | 0.013  | 0.042  | 0.037  |
| Cl | 0.042                                     | 0.055  | 0.013  | 0.045  | 0.037  |
| K  | 0.014                                     | 0.019  | 0.015  | 0.011  | 0.039  |
| Ca | 0.014                                     | 0.019  | 0.012  | 0.010  | 0.015  |
| Ti | 0.005                                     | 0.007  | 0.005  | 0.004  | 0.005  |
| V  | 0.004                                     | 0.005  | 0.004  | 0.003  | 0.007  |
| Cr | 0.004                                     | 0.006  | 0.002  | 0.004  | 0.004  |
| Mn | 0.003                                     | 0.004  | 0.002  | 0.003  | 0.003  |
| Fe | 0.004                                     | 0.005  | 0.001  | 0.004  | 0.002  |
| Ni | 0.002                                     | 0.002  | 0.001  | 0.002  | 0.001  |
| Cu | 0.002                                     | 0.002  | 0.001  | 0.002  | 0.001  |
| Zn | 0.002                                     | 0.003  | 0.001  | 0.002  | 0.001  |
| Br | 0.003                                     | 0.004  | 0.001  | Not measured                                       | 0.001  |
| Pb | 0.003                                     | 0.004  | 0.002  | Not measured                                       | 0.001  |

ED-XRF, energy dispersive X-ray fluorescence; MDL, minimum detection limits; nano-MOUDI, Micro Orifice Uniform Deposit Impactor; NIST, National Institute for Standard and Technology; PIXE, particle-induced X-ray emission; SDI, small deposit impactor.

background spectrum because of the interaction between the X-ray beam halo and the supporting ring.

Once separated from the supporting ring, both coated blank and sampled foils were analysed ( $I = 800 \mu\text{A}$ ,  $HV = 30 \text{ kV}$ ,  $t = 3000 \text{ s}$ , in vacuum analysis, with a thin Ag primary filter) using the sample holder for correct positioning (in the following this ED-XRF configuration will be called SDI set-up). Ten blank foils were analysed to obtain an average blank value, which was subtracted from sampled Kapton® foils. Blank average values and other statistical parameters are reported in Table 2. MDLs were evaluated from the average blank spectrum as done for the NIST standard. Results for the Kapton® foils are reported in Table 1.

The inter-comparison with PIXE was carried out on four SDI series (stages 1–12 for a total of 48 aerosol samples) collected in Florence. They were analysed first at INFN-LABEC by PIXE and then in Milan by the ED-XRF spectrometer in the SDI configuration. The results obtained by the two laboratories were in good agreement (better than 10%) for most of the detected elements (Fig. 4).

#### Set-up for nano-MOUDI™ samples and inter-comparison with PIXE

The identification of the beam spot was carried out using GAFCHROMIC® films. However, because of the larger area of the aerosol deposit in the nano-MOUDI™ (for most stages the maximum diameter of the sampled area was 16 mm) with respect to the SDI one, an additional test was performed in the Genoa laboratory to be sure to fully irradiate the sampled area. A Ca disk with 16-mm diameter was irradiated and the collimators on the detector were changed (with increasing diameters), until no increase in Ca counts was detected.

The uniformity of the X-ray spot in the irradiated area was scanned using an Sn point-like probe material (resolution:

$3 \times 3 \text{ mm}^2$ ) and the final configuration with a 14-mm diameter collimator on the X-ray tube and 12-mm collimator on the detector was fixed for the analysis of nano-MOUDI™ samples. Owing to the size and the characteristics of the nano-MOUDI™ collecting foils (polycarbonate filters with a 47-mm diameter), no sample holder was needed. Indeed, samples with this size can be directly placed on the bottom of the irradiation chamber, as near as possible to the X-ray tube and the detector. Reproducible sample positioning was obtained by marks on the floor of the irradiation chamber.

The Genoa laboratory had no MICROMATTER™ standards with dimensions similar to the nano-MOUDI™ sampled area and a multi-elemental secondary standard was suitably realised. It consisted of a 24-h PM10 sample collected on a 47-mm diameter filter, which had been previously analysed with the irradiation conditions usually applied by this laboratory for obtaining elemental concentrations in aerosol samples.<sup>[23]</sup> This sample was then punched to obtain a 16-mm diameter area and analysed using the nano-MOUDI™ set-up conditions ( $I = 800 \mu\text{A}$ ,  $HV = 30 \text{ kV}$ ,  $t = 3000 \text{ s}$ , in vacuum analysis with a thin Ag primary filter) to obtain the sensitivity curve. As Br and Pb concentrations were lower than MDL in the secondary standard, the sensitivity for these elements could not be calculated and they were not quantified in the nano-MOUDI™ configuration.

The conditions for the ED-XRF analysis of  $Z > 15$  elements were the same for both the secondary standard and the nano-MOUDI™ samples. In the Genoa laboratory, the concentration of light elements ( $11 < Z < 15$ ) was also measured as the rotation during the sampling produces thin deposits. In this case, self-attenuation effects depend only on the size of aerosol particles<sup>[29]</sup> and the comparison with PIXE is more robust as affected by the same effect. However, in this work no correction for self-attenuation effects was applied. Low-Z elements were analysed with  $I = 150 \mu\text{A}$ ,

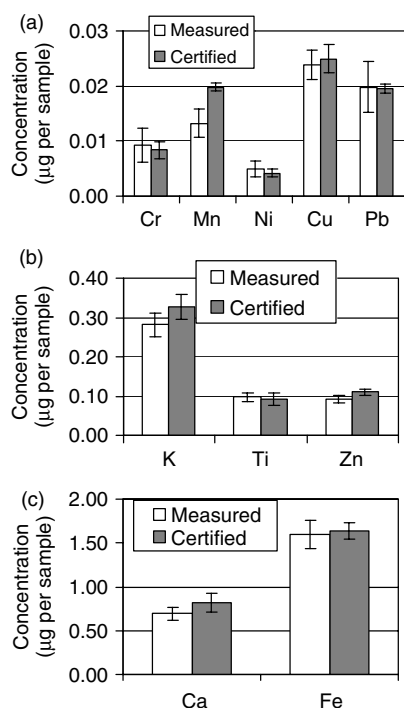


**Figure 3.** Comparison between elemental concentration given by NIST (error bars represent NIST certified uncertainties) and measured by ED-XRF in SDI configuration (error bars are calculated propagating the statistical uncertainty on counts area and the certified 5% uncertainty on MICROMATTER™ standard concentrations). (a) Certified concentration  $< 0.05 \mu\text{g sample}^{-1}$ ; (b)  $0.05 \mu\text{g sample}^{-1} < \text{certified concentration} < 0.40 \mu\text{g sample}^{-1}$  and (c)  $0.40 \mu\text{g sample}^{-1} < \text{certified concentration} < 2.00 \mu\text{g sample}^{-1}$ .

**Table 2.** Statistics on 10 coated Kapton® blanks measured by ED-XRF in the SDI configuration

| Element | $\mu\text{g sample}^{-1}$ |       |       |       |
|---------|---------------------------|-------|-------|-------|
|         | Average                   | SD    | Min   | Max   |
| Cl      | 0.246                     | 0.022 | 0.219 | 0.282 |
| K       | 0.069                     | 0.008 | 0.055 | 0.081 |
| Ca      | 0.443                     | 0.075 | 0.378 | 0.603 |
| Ti      | 0.011                     | 0.002 | 0.008 | 0.014 |
| V       | <MDL                      | <MDL  | <MDL  | <MDL  |
| Cr      | 0.067                     | 0.004 | 0.061 | 0.073 |
| Mn      | 0.026                     | 0.002 | 0.023 | 0.028 |
| Fe      | 0.120                     | 0.010 | 0.111 | 0.141 |
| Ni      | 0.012                     | 0.001 | 0.011 | 0.013 |
| Cu      | 0.016                     | 0.005 | 0.012 | 0.025 |
| Zn      | 0.041                     | 0.004 | 0.035 | 0.047 |

ED-XRF, energy dispersive X-ray fluorescence; MDL, minimum detection limits; SDI, small deposit impactor; SD, standard deviation.

HV = 15 kV,  $t = 2000 \text{ s}$ , in vacuum analysis without primary filter.

MDLs were calculated measuring a set of blank polycarbonate coated filters (Table 1) and applying the same approach described for PIXE. Blank variability (evaluated on 50 blanks) was mainly because of the manual coating operation carried out in the laboratory. Owing to the high blank variability (Table 3), all blanks

**Table 3.** Statistics on 50 coated polycarbonate blanks measured by ED-XRF in the nano-MOUDI™ configuration

| Element | $\mu\text{g sample}^{-1}$ |       |       |       |
|---------|---------------------------|-------|-------|-------|
|         | Average                   | SD    | Min   | Max   |
| Na      | <MDL                      | <MDL  | <MDL  | <MDL  |
| Mg      | 0.720                     | 0.900 | 0.070 | 2.870 |
| Al      | 0.180                     | 0.110 | 0.090 | 0.460 |
| Si      | 0.520                     | 0.040 | 0.380 | 0.600 |
| P       | <MDL                      | <MDL  | <MDL  | <MDL  |
| S       | 0.624                     | 0.110 | 0.427 | 0.844 |
| Cl      | 0.805                     | 0.442 | 0.060 | 1.156 |
| K       | <MDL                      | <MDL  | <MDL  | <MDL  |
| Ca      | 0.173                     | 0.056 | 0.038 | 0.277 |
| Ti      | 0.013                     | 0.003 | 0.005 | 0.020 |
| V       | <MDL                      | <MDL  | <MDL  | <MDL  |
| Cr      | 0.183                     | 0.027 | 0.128 | 0.220 |
| Mn      | 0.121                     | 0.005 | 0.113 | 0.133 |
| Fe      | 0.263                     | 0.029 | 0.218 | 0.351 |
| Ni      | 0.019                     | 0.003 | 0.015 | 0.025 |
| Cu      | 0.033                     | 0.004 | 0.025 | 0.040 |

ED-XRF, energy dispersive X-ray fluorescence; MDL, minimum detection limits; nano-MOUDI, nano-Micro Orifice Uniform Deposit Impactor; SD, standard deviation.

were analysed before the sampling to perform a sample-by-sample blank correction.

The inter-comparison with PIXE was performed measuring one nano-MOUDI™ series (stages 1–13 + backup, for a total of 14 aerosol samples) collected in Genoa. The samples were analysed first in Genoa by ED-XRF spectrometry and then at INFN-LABEC by PIXE. The results obtained by the two laboratories were in good agreement, better than 10% for most of the detected elements (Fig. 5).

## Discussion

A good correlation between the concentrations measured by ED-XRF and PIXE on both SDI (Fig. 4) and nano-MOUDI™ samples was found (Fig. 5). This result proves that the ED-XRF analysis is able to determine the size-segregated elemental concentration. Only elements detected in very low concentration (e.g. V and Ni) show a lower correlation, although ED-XRF and PIXE values are often comparable when error bars are considered. In fact, significant uncertainties are always registered for low concentration values because of the low counting statistics. The ratio between ED-XRF and PIXE concentration values is generally  $1.0 \pm 0.1$  (Figs 4 and 5). It is noteworthy that the MICROMATTER™ standards used by the three laboratories to calibrate their set-up belong to different batches, each certified within 5%, indicating that not significant systematic discrepancy affects the ED-XRF results. The agreement between ED-XRF and PIXE for Mn data in the SDI data set (Fig. 4) is also noteworthy, suggesting that the disagreement between the ED-XRF result and the Mn value certified by the NIST standard cannot be ascribed to problems occurred to the ED-XRF analysis. In the nano-MOUDI™ results (Fig. 5) Ti, Mn, and Cu results showed a higher slope in the regression line (1.15–1.19). Some discrepancies between ED-XRF and PIXE observed in

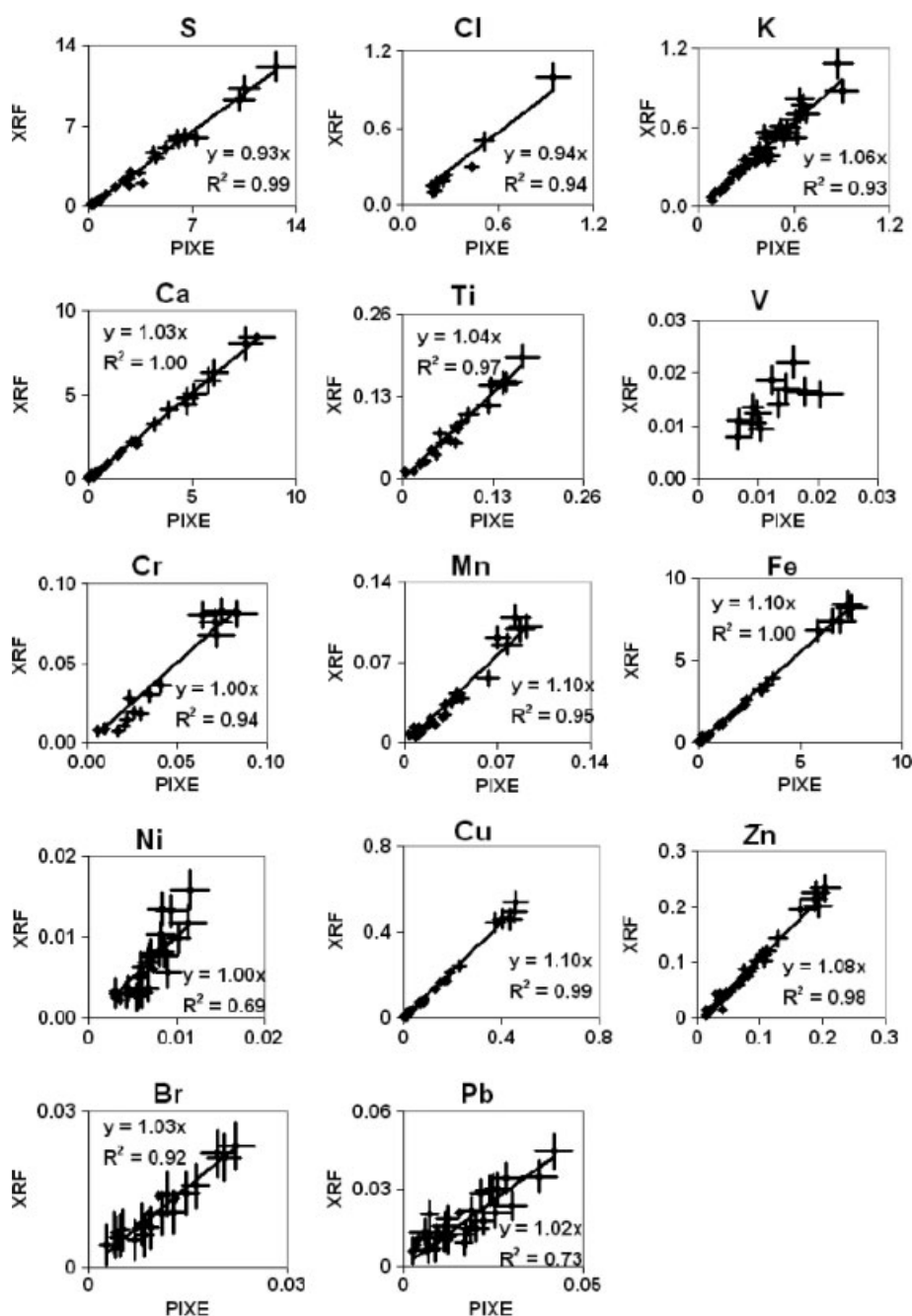


**Figure 4.** ED-XRF versus PIXE values for SDI size-segregated samples. On both axes, elemental concentrations in  $\mu\text{g sample}^{-1}$  are reported.

nano-MOUDI™ results might be because of the use of a secondary multi-elemental standard for ED-XRF calibration.

In Table 2, the variability of coated Kapton® blanks (i.e. SDI sampling foils) is reported; it is generally about 10% with the exception of Ca (17%), Ti (18%), and Cu (31%). To improve the quality of ED-XRF results, a sample-by-sample blank correction would be useful. Unfortunately, in the SDI set-up this is not feasible because it would require a strong collimation of the X-ray beam and very long analysis time to obtain an acceptable counting statistics. Indeed, to perform a sample-by-sample blank correction we should analyse either the Kapton® impaction foils, which are ring supported before the sampling (see Section on Set-up for SDI Samples and inter-comparison with PIXE for related

problems) or a non-sampled part (a region of about  $1 \times 2 \text{ mm}^2$ ) of the Kapton® foil after the sampling (i.e. without the plastic ring).

The good agreement in the inter-comparison results between ED-XRF and PIXE suggests that the blank variability in the SDI set-up does not significantly affect the results.

On the contrary, the nano-MOUDI™ polycarbonate filters are not ring-supported; therefore, the analysis on blank filters can be carried out by ED-XRF before the sampling, improving elements detection and quantification especially in case of low concentrations.

As the focused proton beam used in PIXE can selectively analyse the outer part of the samples (i.e. without particle deposits), a check on possible contaminations that occurred during the

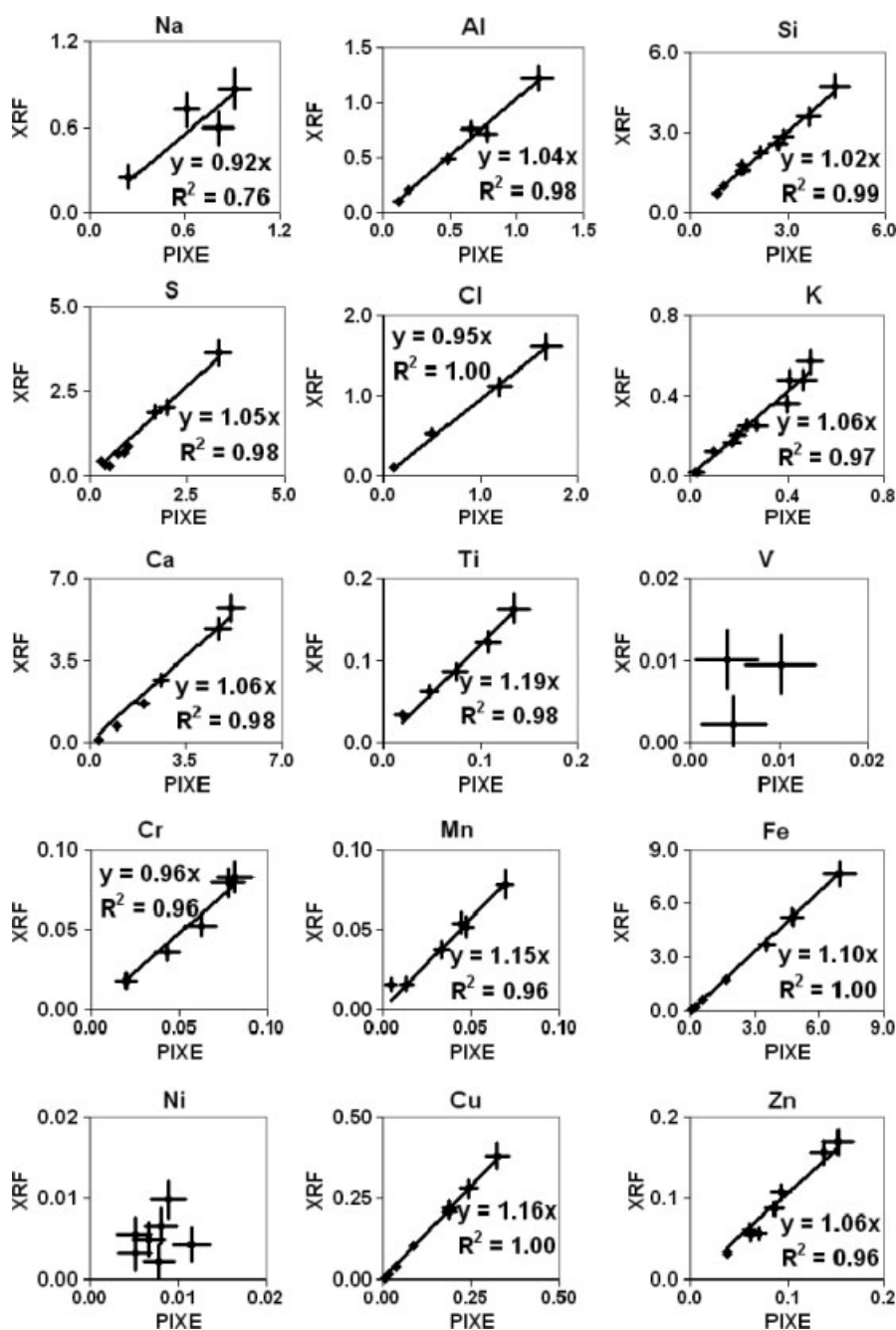


**Figure 5.** ED-XRF versus PIXE values for nano-MOUDI™ size-segregated samples. On both axes, elemental concentrations in  $\mu\text{g sample}^{-1}$  are reported.

sampling (e.g. volatilisation of vacuum grease, back streaming of oil from the vacuum pump, etc.) can also be performed.

## Examples of Application

Preliminary measurements on real samples were carried out using the SDI and nano-MOUDI™ set-up. Only a few examples of the size distributions will be given here, as the detailed analysis of these results is out of the aim of this article.

Size-segregated aerosol samples were collected at urban background sites in the cities of Florence and Milan and at a traffic site in the city of Genoa. In Fig. 6, Fe and Zn size distributions are reported as examples. Fe size distributions are quite similar at

the three sites; there is always a big mode at diameters higher than  $2.5\ \mu\text{m}$ , while the contribution at sizes lower than a few tenths of micrometres is almost negligible. On the contrary, the Zn size distributions obtained in the three cities are completely different. In particular, at the traffic site in Genoa the Zn concentration is higher in the coarse fraction as often reported in the literature.<sup>[30]</sup>

## Conclusions

This work aimed at developing a methodology to analyse aerosol size-segregated samples by ED-XRF spectrometry, which is not customary in this application. In particular, we set up two identical ED-XRF spectrometers to analyse samples collected using



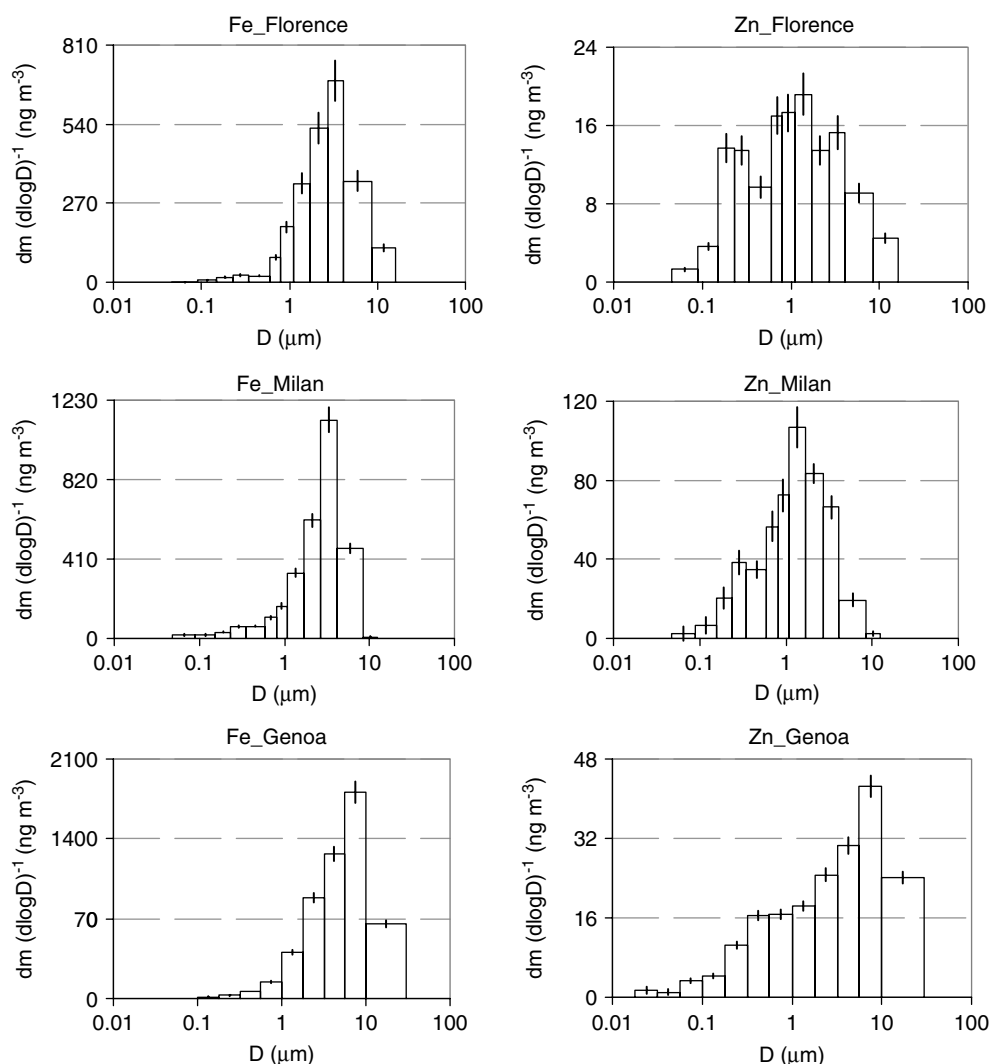


**Figure 6.** Examples of Fe and Zn size distributions measured at Florence (sampled by SDI), Milan (sampled by SDI), and Genoa (sampled by nano-MOUDI™).

two widely used multi-stage cascade impactors (SDI and nano-MOUDI™). The peculiarities of these impactors required slightly different approaches in the ED-XRF set-up and analysis; however, the methodologies here described can be extended to different impactors and/or ED-XRF spectrometers.

Different steps were needed to choose a suitable measurement geometry and determine the sensitivity curve. In particular, the irradiation geometry played a key role because the size-segregated samples are inhomogeneous. The analysis of suitable standards ensured accurate quantitative results without the need for scaling factors as done in a previous work.<sup>[24]</sup>

An inter-comparison with PIXE was carried out to have an additional quality check. The agreement between ED-XRF and PIXE in both the SDI and nano-MOUDI™ set-up was very satisfactory.

As expected, PIXE MDLs were lower than ED-XRF ones, especially for  $Z < 20$ , but we demonstrated that ED-XRF – after a suitable optimisation – can be considered a good alternative to PIXE in the analysis of size-segregated samples. This is noteworthy as ED-XRF is much cheaper, easier to use, and more widespread.

Future developments will face the problem of the quantification of  $11 < Z < 16$  elements, which has been preliminarily carried out for the nano-MOUDI™ samples only.

## Acknowledgements

This research project was funded by the Italian Ministry of Education, University, and Research under the PRIN2007 grant and by the INFN under the NUMEN experiment grant. The Florence group acknowledges the financial support of ST@RT project, promoted by Regione Toscana.

## References

- [1] HEI Review Committee (HEI), *Understanding the Health Effects of Components of the Particulate Matter: Progress and Next Steps*, Health Effect Institute: Boston, **2002**.
- [2] C. A. Pope III, R. T. Burnett, M. J. Thun, E. E. Calle, D. Krewski, K. Ito, G. D. Thurston, *J. Air Waste Manage. Ass.* **2002**, *287*, 1132.
- [3] I. Balász, W. Hofmann, T. Heistracher, *J. Appl. Physiol.* **2003**, *94*, 1719.
- [4] W. Maenhaut, J. Ptasiński, J. Cafmeyer, *Nucl. Instrum. Methods Phys. Res., Sect. B* **1999**, *150*, 422.
- [5] C. A. Pope III, D. W. Dockery, *J. Air Waste Manage. Ass.* **2006**, *56*, 709.
- [6] J. H. Seinfeld, S. N. Pandis, *Atmospheric Chemistry and Physics*, Wiley: New York, **1998**.
- [7] K. L. Dreher, R. H. Jaskot, J. R. Lehmann, J. H. Richards, J. K. Mcgee, A. J. Ghio, D. L. Costa, *J. Toxicol. Environ. Health* **1997**, *50*, 285.
- [8] R. Hillamo, E. I. Kauppinen, *Aerosol Sci. Technol.* **1991**, *14*, 33.

- [9] V. A. Marple, K. L. Rubow, S. M. Behm, *Aerosol Sci. Technol.* **1991**, *14*, 434.
- [10] W. Maenhaut, R. Hillamo, T. Mäkelä, J.-L. Jaffrezo, M. H. Bergin, C. I. Davidson, *Nucl. Instrum. Methods Phys. Res., Sect. B* **1996**, *109/110*, 482.
- [11] J. W. Nelson, G. G. Desadeleer, K. R. Akselsson, J. W. Winchester, *Adv. X-ray Anal.* **1976**, *19*, 403.
- [12] T. A. Cahill, P. J. Feeney, R. A. Eldred, *Nucl. Instrum. Methods Phys. Res., Sect. B* **1987**, *22*, 344.
- [13] K. S. Johnson, A. Laskin, J. L. Jimenez, V. Shutthanandan, L. T. Molina, D. Salcedo, K. Dzepina, M. J. Molina, *Aerosol Sci. Technol.* **2008**, *42*, 6619.
- [14] N. Bukowiecki, M. Hill, R. Gehrig, C. N. Zwicky, P. Lienemann, F. Hegedüs, G. Falkenberg, E. Weingartner, U. Baltensperger, *Environ. Sci. Technol.* **2005**, *39*, 5754.
- [15] I. Salma, R. Ocskay, N. Raes, W. Maenhaut, *Atmos. Environ.* **2005**, *39*, 5363.
- [16] P. M. Grohse. in: *Elemental Analysis of Airborne Particles* (Eds: S. Landsberger, M. Creatchman), Gordon and Breach Science Publishers: Amsterdam, **1999**, p 1.
- [17] M. H. Bergin, J.-L. Jaffrezo, C. I. Davidson, J. E. Dibb, S. N. Pandis, R. Hillamo, W. Maenhaut, H. D. Kuhns, T. Mäkelä, *J. Geophys. Res.* **1995**, *100*, 16275.
- [18] S. A. E. Johansson, J. L. Campbell, *P.I.X.E. A Novel Technique for Elemental Analysis*, John Wiley & Sons: New York, **1988**.
- [19] R. Jenkins, *X-Ray Florescence Spectrometry* (2nd edn), John Wiley & Sons: New York, **1999**.
- [20] P. Van Espen, F. Adams, W. Maenhaut, *Bull. Soc. Chim. Belg.* **1981**, *90*, 305.
- [21] F. Adams, P. Van Espen, W. Maenhaut, *Atmos. Environ.* **1983**, *17*, 1521.
- [22] G. M. Marcazzan, M. Ceriani, G. Valli, R. Vecchi, *X-ray Spectrom.* **2004**, *33*, 267.
- [23] V. Ariola, A. D'Alessandro, F. Lucarelli, G. Marcazzan, F. Mazzei, S. Nava, I. Garcia Orellana, P. Prati, G. Valli, R. Vecchi, A. Zucchiatti, *Chemosphere* **2006**, *62*, 226.
- [24] P. Van Espen, H. Nullens, F. Adams, *Nucl. Instrum. Methods Phys. Res., Sect. B* **1977**, *142*, 243.
- [25] G. Calzolari, M. Chiari, I. Garcia-Orellana, F. Lucarelli, A. Migliori, S. Nava, F. Taccetti, *Nucl. Instrum. Methods Phys. Res., Sect. B* **2006**, *249*, 928.
- [26] J. A. Maxwell, W. J. Teesdale, J. L. Campbell, *Nucl. Instrum. Methods Phys. Res., Sect. B* **1995**, *95*, 407.
- [27] G. Calzolari, M. Chiari, F. Lucarelli, F. Mazzei, S. Nava, P. Prati, G. Valli, R. Vecchi, *Nucl. Instrum. Methods Phys. Res., Sect. B* **2008**, *266*, 2401.
- [28] J. Boman, P. Standzenieks, E. Selin, *X-ray Spectrom.* **1991**, *20*, 337.
- [29] P. Formenti, S. Nava, P. Prati, S. Chevallier, A. Klaver, S. Lafon, F. Mazzei, G. Calzolari, M. Chiari, *J. Geophys. Res.* **2010**, *115*, D01203.
- [30] I. Salma, W. Maenhaut, *Environ. Pollut.* **2006**, *143*, 479.